MULTICOMPONENT DROPLET COMBUSTION AND SOOT FORMATION IN MICROGRAVITY

N96-15558

C. Thomas Avedisian
Cornell University
Ithaca, New York

Introduction

Most practical fuels which are burned in combustion-powered devices, stationary power plants, and incinerators are multicomponent in nature. The differing properties of fuels effects the combustion behavior of the blend. Blending can be useful to achieve desired ends, such as increasing burning rates and reducing extinction diameter and soot formation. Of these, particulate emissions is one of the most important concerns because of its impact on the environment. It is also the least understood and most complicated aspect of droplet combustion. Because of this fact, a well characterized flow field and simplified flame shape can improve the understanding of soot formation during droplet combustion. The simplest flame shape to analyze for a droplet, while still maintaining the integrity of the droplet geometry with its inherent unsteadiness, is spherical with its associated one-dimensional flow field.

This project will concern soot formation in microgravity droplet flames and some parameters that effect it. Because it has not yet begun, this paper will briefly review some related results on this subject.

Experiment

For combustion in an ambience of air (the most practical environment), the pressure must be reasonably high (usually atmospheric or higher) for soot formation to be a factor. Low pressure tends to suppress sooting for an ambience of air. With increasing pressure, buoyancy becomes a factor so a microgravity environment can compensate. In past work, low gravity was realized by conducting experiments on board a drop tower, and both free and fiber-supported droplets were studied. Free droplets were formed and deployed by a piezoelectric droplet generator [1]. For fiber supported droplets, the ratio of the fiber to the droplet diameter at ignition is kept small to minimize the influence of the fiber, which can effect soot patterns as shown in fig. 1 [2]. Burning rates for fiber-supported droplets need to match (within experimental error) the burning rates of unsupported droplets of similar size to avoid a fiber influence on burning. Then, results from fiber supported droplets can be useful for single component fuels.

Typical data are the evolution of the droplet diameter. If the luminous zone is especially pronounced in photographs, the flame 'diameter' can also be measured but few data exist for the flame or luminous zone boundary that spans a significant portion of the burning history. The flame is ideally identified by a peak in a radical species like OH or temperature distribution, but the diagnostics necessary to measure OH distribution around burning droplets have not yet been utilized in microgravity droplet combustion experimentation. In practice, the flame and soot shell diameters are identified from photographs. This type of recording medium will continue to be indispensable for data extraction. Simultaneous measurement of the droplet diameter, D, the mean soot shell diameter, D_s, and the 'flame' diameter, D_f, however, is difficult or impossible if soot image intensity dominates.

Data reduction from the motion picture negatives is via commercial data acquisition software. Sooting is inferred from examination of digitized photographs by scanning the pixels. This method is obviously qualitative but necessary because of the difficulty of employing more quantitative soot diagnostic methods in a drop tower environment.

PRECEDING PAGE BLANK NOT FILMED

Mixtures and Emulsions

Many models have been formulated for spherically symmetric burning of multicomponent fuels, including emulsions, but few relevant data have been published. Combustion of a mixture droplet, especially, can be effected by the experimental method. For fuel blends, fiber supported droplets can effect the species distribution within the droplet, promote heterogeneous nucleation on the fiber surface, and (for an emulsion) cause coalescence of the dispersed phase. Unsupported droplets avoid these effects but it is more difficult to capture their complete combustion history on film because of the necessity of keeping the droplet stationary. Unsupported droplets of methanol/dodecanol, heptane/hexadecane, and methanol/toluene have been examined in microgravity [3-6]. Some of the observations showed multistage combustion and microexplosions, and an influence of composition on soot formation.

Concerning emulsions, two studies are known for microgravity droplet flames [7,8]. Emulsions of water and oil, and hydrazine and oil, were examined [8] using the suspended droplet technique in which disruptions akin to microexplosions were noted. For the present project, emulsions using free droplets will be studied. The continuous phase will be heptane and the dispersed phase will be water. Water is selected as the dispersed phase because of its expected influence on soot formation through the flame temperature. Heptane as the continuous fuel phase permits referencing the results with microgravity heptane droplet flames. The similar volatility of heptane and water should not lead to microexplosions. The presence of a low volatility surfactant that is usually needed to stabilize an emulsion, however, will be assessed in the experiments.

Evolution of the Flame and Soot Shell 'Diameter'

The appearance of a ring of soot or 'shell' is unique to spherical droplet flames for sooting fuels. In a convective environment, soot entrapment will also occur but the soot pattern shape will roughly follow that of the flame which is stretched out in a tear-drop shape. First observed by Okajima and Kumagai [9], spherical soot patterns formed between droplet and flame have been more prominent in recent studies. The shell of soot will form where the forces acting on the aggregates balance. Thermophoretic forces on aggregates are directed toward the flame. The force due to Stefan drag is directed away from the droplet. The 'shape' of the shell is dictated by the velocity distribution around the droplet which is spherical for a purely radial flow field.

The time dependence of D_s (the shell "diameter" really has a finite thickness) reflects the temporal variation of D_f during burning. An example is illustrated in fig. 2a, where the evolution of D_s/D is shown for n-heptane [1] and compared with measurements of the outer luminous zone, D_f/D, which is here taken to be the flame diameter. Similar results for a 1-chloro-octane (CHC) flame are also shown in fig. 2b. That both D_s/D and D_f/D track together, with $D_s/D<D_f/D$ as shown in fig. 2, is consistent with the fact that soot precursors form on the fuel rich side of the flame. Based on the time dependence of D_f/D shown in fig. 2, 'quasi-steady' droplet combustion which requires D_f/D to be constant [10] is not realized in the experiments.

Effect of Droplet Diameter on Soot Formation and Burning Rate

The evidence for this effect is qualitative because it is based on subjective judgements from comparing intensities of photographs for droplets of different size. Generally, smaller droplets show less intense soot images than large droplets. Fig. 3 shows four different fiber-supported heptane droplets under similar backlighting conditions [1]. The fiber diameter was 30μm for the two smallest droplets and 50μm for the two largest droplets. The initial (equivalent) diameters range from .44mm to 1.01mm and the value of t/D_o^2 is approximately the same to facilitate comparisons. Differences in soot image intensity are evident.

The mass of soot formed during droplet combustion should increase as the initial droplet diameter increases because of the larger mass of fuel vaporized. Less clear is whether or not the 'proportional' amount of soot formed, that is the amount of soot formed per unit mass of fuel vaporized, is effected by droplet size. No measurements of this quantity have been made for spherical droplet flames. However, for droplets burning in a convective environment, the amount of

soot formed per unit mass of fuel burned appears to increase as the droplet diameter increases and to scale as D^n [11] where $3<n<4$.

Concerning the burning rate, some evidence exists to show that the droplet burning rate is influenced by D_o [1]. Fig. 4 shows how K ($\equiv - d(D^2)/dt$) varies with D_o for heptane (for two-spark ignition) for $.4mm<D_o<1.1mm$. K increases as D_o decreases, which is not consistent with the classical theory of droplet combustion [10] which, though, neglects soot formation.

Soot formation can cause K to change continuously during burning. Aggregates formed in the early of burning where the droplet diameter is largest will become trapped between the droplet and flame. In the later period where the droplet diameter is considerably reduced from the initial value, proportionally less soot should be produced. However, entrapped aggregates from the earlier period of burning can still remain near the droplet late in the burning history. Also, the heat generated at the flame (relative to the droplet size) should increase proportionally as diameter is reduced because proportionally fewer fuel molecules are converted to soot if smaller droplets soot proportionally less than larger ones. As a result, K could progressively increase as burning proceeds. The evidence for this effect is circumstantial as shown in fig. 5 for CHC [1], but it does suggest a more constant K for smaller, less sooting, droplets than larger ones. Variations in K during burning can be difficult to identify because it requires obtaining second derivatives which can greatly magnify data uncertainty. The early period of burning (the first 10% of it or so), and the end of burning where the droplet diameter can be too small, can be difficult to resolve using conventional photographic means. There will continue to be a need for increased precision of droplet diameter measurements.

The residence time of fuel molecules on the fuel-rich side of a flame can be used to explain qualitatively trends shown in fig. 3. The longer fuel molecules reside on the fuel rich side of the flame the greater will be the probability of their ultimate conversion to soot aggregates. Two characteristic times are the transport time of fuel molecules between the droplet and flame (D_o^2/α) and a pyrolysis reaction time. The ratio of these two times, τ, is $\tau \equiv AD_o^2\exp[-E/(RT)]/\alpha$ [12] where E is an activation energy associated with a first order pyrolysis reaction, A (s^{-1}) is the corresponding pre-exponential factor for an Arrenhius rate constant, and α is a mean gas diffusivity. The propensity for soot formation increases as conditions are adjusted to increase τ, and vice versa for decreasing values of τ. Trends based on this proportionality are consistent with experimental observations. For example, decreasing D_o lowers τ which should lower the propensity to soot. This is consistent with experimental results [1,11].

Modelling

Soot formation processes have not yet been included in a model for droplet combustion. Such things as complex chemistry, the steps and associated rates for forming soot aggregates, soot aggregate entrapment, and the effect of converting fuel molecules to soot on the heat release at the flame would have to be included in a detailed model. Some of the building blocks for detailed modelling have been developed in past research, for example the influence of flame radiation [13,14], complex chemistry for several fuels [15-17], the forces acting on soot aggregates [17,18], and models for soot production rates in flames [19-21].

If soot formation is not accounted for, the resulting analysis will be of limited applicability, for example to a small droplet or low pressure limit where soot formation is minimal. Such a limit was assumed for a spherically symmetric flame for quasi-steady conditions and neglecting flame radiation [17]. Complex chemistry for heptane [22] was, however, included in the model. The temperature and velocity distributions calculated from this model were used to predict the net force ζ on particles (due to thermophoresis and the Stefan drag force) for a fictitious situation in which the soot particles do not influence the transport processes. Fig. 6 [17] shows two equilibrium positions for particle entrapment for a given particle radius, r_p, but only one of them is stable: the one closest to the droplet. Concerning a soot precursor species, fig. 7 [17] shows that the calculated mass of

acetylene formed per mass of fuel vaporized decreases as the initial droplet diameter decreases.

Summary and Future Work

Past research has shown that composition and droplet size can influence the droplet burning rate and soot formation for near spherically symmetric burning. Future work will extend the range of droplet diameters to smaller droplets than has been examined in a near convection-free environment, compare the results to a nonsooting fuel for referencing, and extend the analysis for sooting fuels. The experiments will also include study of emulsions using free droplets to examine the effect of water. Metal-based additives may also be examined because of their known role of influencing soot formation in some cases by the effect of the ions produced.

references

1. Jackson, G.S. and Avedisian, C.T. *Proc. R. Soc. Lond.*, **A446**, 1994, 255-276
2. Wellin, J.D., Jackson, G.S. and Avedisian, C.T. paper no. 88, Fall Eastern States Section Meeting of the Combustion Institute, Princeton, N.J. October 25-27, 1993.
3. Yang, J.C., Jackson, G.S. and Avedisian, C.T. *23rd Symp. (Int.) Comb.*, Pittsburgh, Pa.: The Combustion Institute, 1990, pp. 1619-1625 .
4. Mikami, M., Kono, M., Sato, J., Dietrich, D.L. Williams, F.A. *Com. Sci. Tech.* **90**, 1993, 110-123.
5. Yang, J.C. and Avedisian, C.T. *22nd Symp. (Int.) on Combust.*, Combustion Institute, 1989, pp. 2037-2044
6. Jackson, G.S., Avedisian, C.T., and Yang, J.C. *Proc. R. Soc. Lond.*, **A435**, 1991, 359-369.
7. Okajima, S., Kanno, H., and Kumagai, S. *Acta Astronaut.* **12**, 1985, 555-563.
8. Kimura, M., Ihara, H. Okajima, S., and Iwama, A. *Comb. Sci. Tech.*, **44**, 1986, 289-306.
9. Okajima, S. and Kumagai, S. *15th Symp. (Int.) Comb.*, Pittsburgh, Pa.: The Combustion Institute, 1975, pp. 401-407.
10. Glassman, I. *Combustion*, 2nd ed., Orlando, Fla.: Harcourt, Brace, Jovanovich, 1987.
11. Gupta, S.B., Ni, T. and Santoro, R.J. paper no. 50, Fall Eastern States Section Meeting of the Combustion Institute, Cearwater Beach, Fl., December 5-7, 1994.
12. Avedisian, C.T. *Comb. Sci. Tech Book Series*, vol. 2, in press.
13. Lage, P.L.C. and Rangle, R.H. *J. Thermophys. Heat Transf.* **7**, 1993, 101-109.
14. Saitoh, T., Yamazaki, K. and Viskanta, R. *J. Thermophys. Heat Transf.* **7**, 1993, 94-100.
15. Cho, S.Y., Choi, M.Y., and Dryer, F.L. *23rd Symp. (Int.) Comb.*, Pittsburgh, Pa.: The Combustion Institute, 1990, pp. 1611-1617.
16. Cho, S.Y., Yetter, R.A., and Dryer, F.L. *J. Comp. Phys.*, **102**, 1992, 160-179.
17. Jackson, G.S. and Avedisian, C.T. *AIAA* paper no 95-0286, 1995.
18. Jackson, G.S, Avedisian, C.T., and Yang, J.C. *Int. J. Heat Mass Trans.*, **35** (8), 1992, 2017-2033.
19. Kesten, A.S., Sangiovanni, J.J. and Goldberg, P. *J. Eng. for Power*, **102**, 1980, 613-618.
20. Kennedy, I.M., Kollman, W. and Chen, J.Y. *Comb. Flame.* **81**, 1990, 73-85.
21. Frenklach, M. and Wang, H. 1990 *23rd Symp. (Int.) Comb.*, Pittsburgh, Pa.: The Combustion Institute, 1990, pp. 1559-1566.
22. Warnatz, J. *20th Symp. (Int.) Comb.*, Pittsburgh, Pa.: The Combustion Institute, 1984, pp. 845-856.

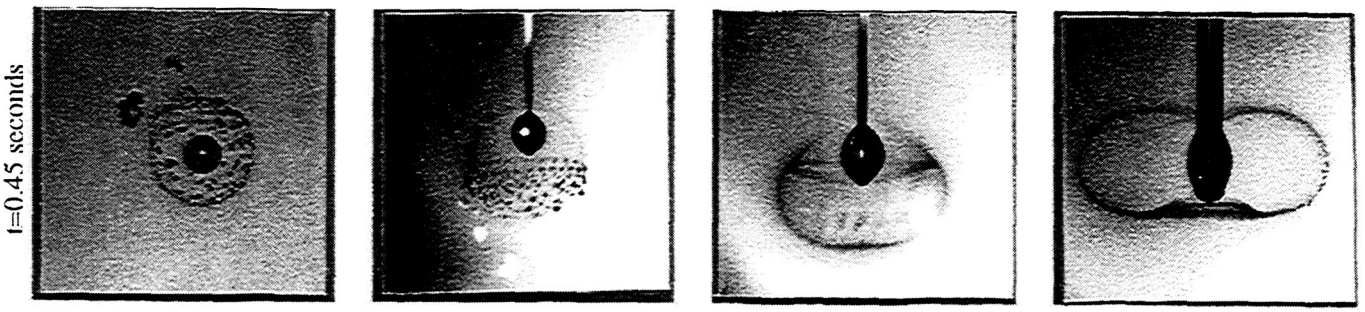

Figure 1: Effect of support fiber diameter on soot patterns and droplet shape .45s after ignition. a) free droplet; b) .057μm fiber, D_o=700μm; c) 110μm fiber, D_o =770μ; d) 330μm fiber, D_o=610μm

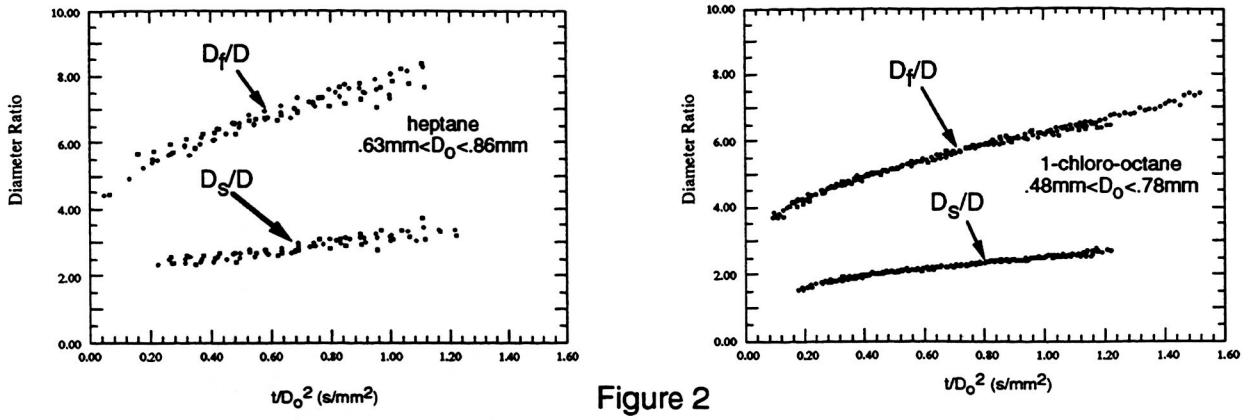

Figure 2

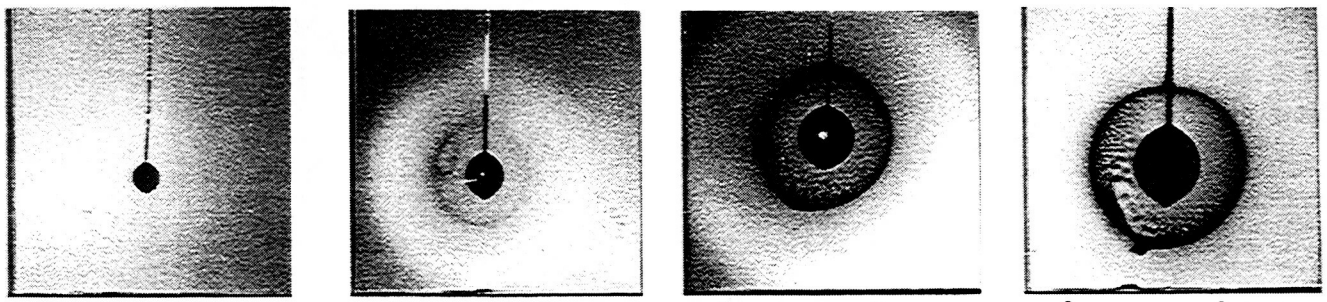

Figure 3: Effect of D_o on soot image intensity for suspended heptane droplets.

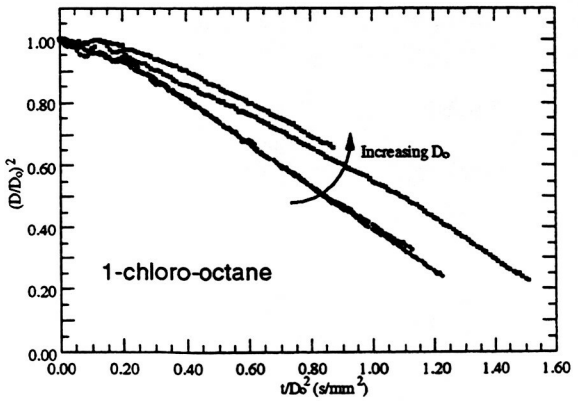

Figure 4

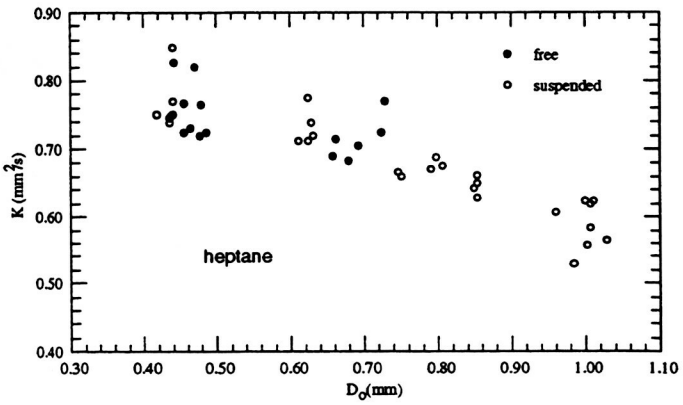

Figure 5

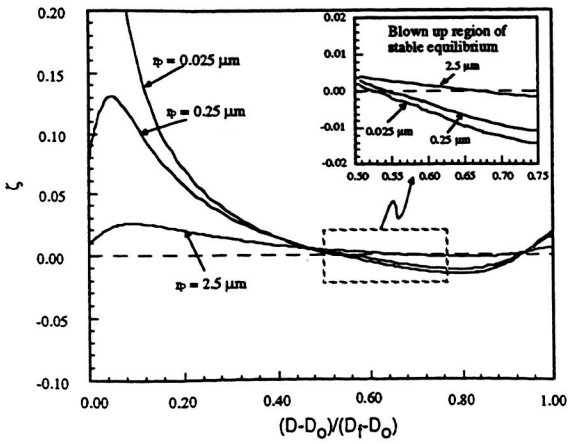

Figure 6

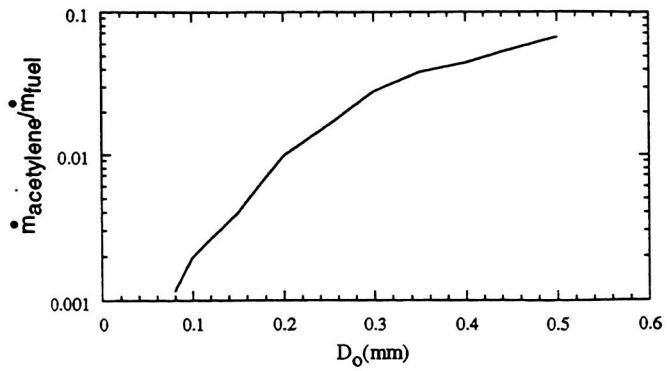

Figure 7